Biological Trace Element Research (2019) 189:209–223
https://doi.org/10.1007/s12011-018-1441-8

Transcriptional Study Revealed That Boron Supplementation May Alter the Immune-Related Genes Through MAPK Signaling in Ostrich Chick Thymus

Ke Xiao[1] · Keli Yang[1] · Jing Wang[1] · Pengpeng Sun[1] · Haibo Huang[1] · Haseeb Khaliq[1] · Muhammad Ahsan Naeem[1] · Juming Zhong[2] · Kemei Peng[1]

Received: 12 May 2018 / Accepted: 10 July 2018 / Published online: 9 August 2018

Abstract

The objective of this study is to construct a digital gene expression tag profile to identify genes potentially related to immune response in the ostrich. Exposure to boron leads to an immune response in the ostrich, although the underlying mechanism remains obscure. Thus, a dire need of biological resource in the form of transcriptomic data for ostriches arises to key out genes and to gain insights into the function of boron on the immune response of thymus. For this purpose, RNA-Seq analysis was performed using the Illumina technique to investigate differentially expressed genes in ostrich thymuses treated with different boric acid concentrations (0, 80, and 640 mg/L). Compared with the control group, we identified 309 upregulated and 593 downregulated genes in the 80 mg/L treated sample and 228 upregulated and 1816 downregulated genes in 640 mg/L treated sample, respectively. Trend analysis of these differentially expressed genes uncovers three statistically significant trends. Functional annotation analysis of the differentially expressed genes verifies multiple functions associated with immune response. When ostrich thymuses were treated with boron, expression changes were observed in genes predominantly associated with MAPK and calcium signaling pathways. The results of this study provide all-inclusive information on gene expression at the transcriptional level that further enhances our apprehension for the molecular mechanisms of boron on the ostrich immune system. The calcium and MAPK signaling pathways might play a pivotal role in regulating the immune response of boron-treated ostriches.

Keywords Ostrich thymus · Boron · Transcriptome · Immune response · MAPK

Introduction

African ostrich (*Struthio camelus*), the oldest member of the ratite lineage, is one type of flightless bird that is regarded as a living fossil of primitive birds and is a model for evolutionary research of ancient ratites [1, 2]. In recent years, the ostrich has garnered significant economic importance as a farmed bird in many counties other than South Africa, including the USA, Australia, China, Canada, New Zealand, Israel, and Europe [3]. An increased demand for ostrich products has drawn attention to its reportedly low productivity in the industry, which generally appears to be due to a high mortality rate attributed to various infections, dehydration, high humidity, less floor space, diseases or stressors, and nutritional imbalance, particularly within the first 3 months of age [4–6]. The growth of ostrich chicks is balanced against their immune function, an important survival trait [7].

Boron being an essential micro-mineral for animals and humans [8] is known for its important role in the immune system [8], the endocrine system, and in mineral metabolism [9, 10]. The previous researches have proved that high doses of boron supplementation caused damage in the kidney [11], bone [12], intestine [13], brain [14], spleen [15], and thymus

Electronic supplementary material The online version of this article (https://doi.org/10.1007/s12011-018-1441-8) contains supplementary material, which is available to authorized users.

✉ Kemei Peng
kemeip@163.com

Ke Xiao
xke1995@126.com

[1] College of Veterinary Medicine, Huazhong Agricultural University, Wuhan 430070, Hubei, People's Republic of China

[2] College of Veterinary Medicine, Auburn University, Auburn, AL 36849, USA

[10] in ostrich, whereas boron benefits at low doses of induction in the biological system. Several lines of evidence indicate that boron is important for normal immune function and responses. Appropriate doses of boron can significantly improve immune function and responses during the late developmental stage of the chicks [9]. However, higher doses of boron can be toxic. Toxic doses of boron can significantly inhibit the development of the central and peripheral immune organs. Previously, Xiao et al. demonstrated that 80 mg/L boric acid can promote the expression of Foxn1 within the ostrich thymus. In contrast, 640 mg/L boric acid can inhibit Foxn1 expression [10]. Thus, boron appears to regulate the immune function of the ostrich thymus. However, the detailed mechanism of action of boron on immune function or response remains obscure.

MAPK, a highly conserved mitogen-activated protein kinase, is one of the most important regulatory mechanisms in eukaryotic cells. MAPK has previously been cloned and categorized within the following five subfamilies: extracellular signal-regulated kinases 1 and 2 (ERK1/2), c-Jun NH2-terminal kinases (JNK1/2/3), p38MAPK (p38 α, β, γ, and δ), and ERK5/BMK1 [16]. The MAPK signaling pathway can mediate fundamental biological processes and cellular responses to external stress signals, such as inflammation, stress, cellular growth and development, differentiation, and apoptosis [17].

MAP kinases play impact essential roles in maintaining the homeostasis of the immune system, from the innate to adaptive immune systems, and from the initiation of immune responses to activation of programmed cell death [18–20]. The most extensively studied MAPK groups are ERK1/2, JNKs, and p38MAPK. The ERK pathway is involved in the regulation of cell growth, cell progression, and apoptosis [16, 20]. Moreover, the Ras-ERK pathway is required for T cell activation [14, 20], thymocyte development [21, 22], and apoptosis. The JNK pathway is strongly activated in response to cytokines and stress [23] and can mediate cell differentiation and cell death [24]. The JNK pathway is also activated during innate immune responses and plays an important role in regulating the generation of thymic T cells and the activation, differentiation, and death of T cells in the peripheral immune system [18]. The p38MAPK kinase pathway is associated with inflammation, cell growth, differentiation, and cell death [25]. In addition, p38 activity is crucial for normal immune and inflammatory response [26, 27]. In the immune system, the p38MAPK kinase pathway has been implicated in the regulation of innate and adaptive immunity [18, 28]. The JNK and p38MAP signaling pathways are known to regulate T cells and to play an important role in thymic development and Th1/Th2 differentiation [18]. Taken together, both boron and the MAPK signaling pathways can regulate immune responses in the thymus. However, it is unclear whether boron regulates immune responses via the MAPK signaling pathway. The role of boron has been well-reported in regulation of immune response in rats, mice, and the Gushi chick. However, its role in African ostrich thymus is still poorly understand. Therefore, we have investigated potential mechanisms underlying the boron-mediated regulation of the immune response in thymus of African ostrich in the current study.

In recent years, high-throughput sequencing techniques become a powerful, efficient, and economical tool [29–31], that is widely used in gene discovery [32, 33], transcriptomic research [34], gene expression analysis [35, 36], and other screening research. As a consequence, the ostrich genome sequence has been published and annotated. However, less is known about the transcriptional networks that are related to the effects of boron in the regulation of ostrich immunity. In this study, we examined thymuses from the ostriches treated with different doses of boron and used the RNA-Seq analysis to test for differences in the expression of genes in ostrich thymuses during boron treatment. RNA-Seq analysis was performed using Illumina technology, provided comprehensive information about gene expressions at the transcriptional level to widen our understanding of the molecular mechanisms of boron on the ostrich immune system.

Materials and Methods

Animal Feed, Sample Preparation, and Collection

Thirty healthy 1-day-old ostrich chicks with similar body size were divided into six groups. Boric acid was added to the distilled drinking water at different dosages for different groups (group I, 0 mg/L; group II, 40 mg/L; group III, 80 mg/L; group IV, 160 mg/L; group V, 320 mg/L; group VI, 640 mg/L), where group I was considered as the control group. The ostrich feeding and administration procedures were performed according to detailed procedure given in our previous study [10, 37]. Apart from boric acid supplementation in the drinking water, the ostrich chicks were fed with a conventional diet for 90 days. After 90 days, the chicks were weighed after a fasting period of 24 h. The final body weight, average daily gain, and average daily feed intake were measured as in our previous study [37]. The thymus samples were collected at 90 days from the different groups and stored at − 80 °C.

RNA Extraction, Library Construction, and Sequencing

As in our previous study, groups I (control, 0 mg/L), III (B80, 80 mg/L), and VI (B640, 640 mg/L) specimens were selected for the RNA-Seq analysis [10]. The total RNA of each of specimen was extracted using Trizol (Invitrogen, USA) according to the manufacturer's protocol. RNA purity was

assessed using a NanoDrop 2000 spectrophotometer (Life Technologies), where the standards applied were as follows: $1.8 \leq OD_{260/280} \leq 2.2$ and $OD_{260/230} \geq 1.8$. RNA quality (RNA integrity number > 6.5) was verified using a Bioanalyzer 2100 system (Agilent Technologies, Santa Clara, CA) and also verified by 1% RNase-free agarose gel electrophoresis. Equal amounts of total RNA (1 μg) were taken from each sample within the same group and pooled together to construct cDNA libraries.

RNA-seq library preparation and sequencing was performed out by Gene Denovo Co. (Guangzhou, China). Briefly, total mRNA was isolated using Oligo-dT beads (Qiagen) and broken into short fragments. Reverse transcription with random primers was used to synthesize first-strand cDNA. Second-strand cDNA was synthesized using DNA polymerase I and RNase H. Short cDNA fragments were purified using the Qia Quick PCR extraction kit (Qiagen, USA), with end reparation and poly (A) addition. After agarose gel electrophoresis, the cDNA fragments were excised and purified for PCR amplification. Lastly, the cDNA libraries were sequenced using Illumina sequencing platform (Illumina HiSeq™ 2000, San Diego, USA) with paired-end sequencing technology (Guangzhou, China); the read length was designated at 90 nt. All raw sequencing data are available from the NCBI Short Read Archive (SRA) with the following accession numbers (SRR 2097530, SRR 2097529, and SRR 2093956).

Data Filtering, Mapping Reads, and Identifying Transcriptome Contents

The sequences generated were subjected to an initial filtering process. Raw reads were trimmed by removing adapter sequences, ambiguous nucleotides, and low-quality reads, and the resulting high-quality sequences were used in subsequent analysis. The clean reads were mapped into the ostrich genome database using SOA Paligner/soap2 software. Not more than two mismatch bases were permitted, and unique mapped reads were obtained. After mapping, the gene expression levels were quantified by simply dividing the number of reads mapped to each gene by the size of its transcripts (known as reads per kilobase of transcript per million mapped reads (RPKM)) and were presented as the distribution of gene coverage, for all 16,560 annotated ostrich genes in the database (Table S1).

RNA-Seq Data Enrichment Analysis

Differentially expressed genes (DEGs) were evaluated among the control, B80, and B640 libraries according to the method described by Audic et al. [38], and DEGs were clustered by Short Time-series Expression Miner (STEM, version 1.2.2b) software [39]. The clustered profiles with P value ≤ 0.05 were considered as significantly expressed. A false discovery rate (FDR) was used to determine the threshold of the P value in multiple tests. In this study, a FDR < 0.05 and a value of the $|\log2\ FC| > 1$ were used as the threshold to judge the significance of differences in gene expression. Gene ontology enrichment analysis of functional significance was applied to map all DEGs to terms in the GO database, which accept the corrected P values (≤ 0.05) as a threshold. Enriched Kyoto Encyclopedia of Genes and Genomes (KEGG) pathways with a P value ≤ 0.05 were significantly enriched in RNA-Seq data. Lastly, the differentially expressed genes were subjected to GO and KEGG pathway analysis to determine possible related functions (GO databases: http://www.geneontology.org/; KEGG Orthology databases: http://www.genome.ip/kegg/) [40].

Quantitative Real-Time PCR Validation of the RNA-Seq Data

The transcription of 20 selected candidate genes was determined using quantitative real-time PCR. First-strand cDNA was generated from 1 μg of total RNA isolated from the ostrich thymus using the HiScript® II Q Select RT SuperMix for qPCR (+gDNA wiper). Primers for quantitative real-time PCR were designed using Primer 3(v.0.4.0) http://bioinfo.ut.ee/primer3-0.4.0/, tested by primer blast and synthesized by TsingKe Biotech Co., Ltd. (Beijing). Ostrich GAPDH (GenBank accession number: XM_009685091.1) was used as a reference. All of the primers were designed for genes of interest are shown in Table 1. Real-time PCR was performed on a Bio-Rad iQ5 Optical System Real-Time PCR System (Bio-Rad, USA) according to the manufacturer's protocol. Each reaction mixture was 20 μL containing 2 μL of diluted first-strand cDNAs and 0.4 μL 10 μM of each primer, SYBR Green PCR Master Mix (Vazyme, Nanjing) 10 μL. Each real-time analysis was performed in triplicate. Expression levels of the target genes were determined by CT values and calculated by $2^{-\Delta\Delta CT}$.

Western Blot Analysis

Proteins were isolated from thymus using RIPA buffer (Boston BioProducts, USA) which was supplemented with Halt™ Protease Inhibitor Cocktail (Thermal Scientific, USA) and 1% PMSF. Protein concentrations were measured using a BCA Protein Assay Kit (Pierce Biotechnology, USA). Equal amounts of total protein were loaded onto 12% PAGE (PPPP3CA, PPP3R1, ERK, p-ERK) or 10% PAGE (p38, p-P38, JNK, p-JNK) and transferred to a PVDF membrane (Merck Millipore, USA). The membranes were incubated with the primary antibodies against ERK1/2 Polyclonal Antibody (Rabbit 1:5000) (Proteintech™, Cat. No 16443-1-

Table 1 The primers designed for qRT-PCR

Gene	Forward primer(5′ → 3′)	Reverse primer (5′ → 3′)	Length (bp)
RAS	5′-GCTGGTGGTGTAGGCAAGAG-3′	5′-CAAGAGGCAGGTTTCTCCAT-3′	129
JNK	5′-GCTCCTCCACCTCAAATCTATG-3′	5′-CCACACCATTCTTGCTTCTTTC-3′	121
ERK	5′-CTCAGCACCTCAGCAACGAT-3′	5′-AACACGAGCCAGTCCAAAGT-3′	167
P38	5′-GGACCTGAAGCCAAGTAACC-3′	5′-TCCAACAGACCAGATGTCAA-3′	184
RSK2	5′-GACTGGTGGTCTTTTGGTGTTT-3′	5′-CCTAATCTGTTTGCTGGGTTTC-3′	188
PKA	5′-ACAGCCACAGCACTACAGAGAC-3′	5′-CCATAGGACAGCAAGTTCAGAG-3′	135
PPP3CA	5′-TGAAAGCGTGCTGACACTGAA-3′	5′-GAGATTGCCTTGTTGATGGAG-3′	228
PPP3R1	5′-GGTCTCCCAGTTCAGTGTCA-3′	5′-GCCTCCTACAACAGCACAGA-3′	244
NFAT-2	5′-ATTCGCTGGTGGTTGAGATA-3′	5′-TGGAACATTAGCAGGAAGATAG-3′	137
MEF2C	5′-TCTCCCTGCCTTCTACTCAA-3′	5′-TCTTCTCGGTCACTTCCATC-3′	175
EGFR	5′-TACCTTCTCAACTGGTGTGTGC-3′	5′-GCGTGATACTCTTTCTCGTCAG-3′	176
IL1R2	5′-CTTACAGTTGGGGAGCGACA-3′	5′-CTTCCTGCTTGACCCTTGTT-3′ ′	166
CIITA	5′-TCAAGAGGGAAGCAATGAGG-3′	5′-CACTGTCTGAGCAACGAGGA-3′	122
FLT3	5′-AACGATAGCGGACATTACACC-3′	5′-AGCAAAACTCCTCTTCACCAA-3′	136
FGL2	5′-CATCAGGAAACTGTGGAGCATA-3′	5′-CCATTGCGAACACCTTTGTATT-3′	112
EDAR	5′-CACAAAGACTGCGAGGGATT-3′	5′-CAAGCACGAGTAGCAAACCA-3′	150
TLR2	5′-TGGTCATTCTCGTCCTTGTG-3′	5′-TGATGTTTTCCACCCAGTCA-3′	177
TLR4	5′-TCGGCTCTCCTTCACCAAAT-3′	5′-GGTAGGAGCCAGGACCAATT-3′	173
FLIP	5′-GCTCTTGTGATTGACCTGGAG-3′	5′-GCTGAGAATGAACGGAGGAC-3′	154
IAP	5′-GCGAAGGCTGGATTTTATTACC-3′	5′-TTAGGAAAGTGTCTCCGATGCT-3′	125
GAPDH	5′-TGGCATACACAGAGGACCAG-3′	5′-ACCAGGAAACCAACTTCACG-3′	185

AP), Phospho-p44/42 MAPK (ERK1/2) Rabbit mAb (Rabbit 1:2000) (Cell Signaling, Cat. No #4370), p38 (V318) pAb (Rabbit 1:800) (Bioworld, Cat. No BS1681), p-p38/MAPK14 (pY322) pAb (Rabbit 1:1000) (Bioworld, Cat. No BS6381), JNK (D-2) (mouse 1:300) (Santa Cruz, Cat. No sc-7345), p-JNK (G-7) (mouse 1:300) (Santa Cruz, Cat. No sc-6254), PPP3CA Polyclonal Antibody (Rabbit 1:2000) (proteintech™, Cat. No 13422-1-AP), PPP3R1 Polyclonal Antibody (Rabbit 1:500) (proteintech™, Cat. No 13210-1-AP), GAPDH (Rabbit 1:1000) (Hangzhou Goodhere, AB-P-R 001), and the matching secondary antibody (peroxidase-labeled anti-mouse IgG or anti-rabbit IgG; 1:50000) (Boster, China). The antibody-specific protein was visualized by ECL detection system.

Results

RNA-Seq Data Evaluation and Analysis

Libraries produced from the total RNA isolated from ostrich thymuses treated with different boric acid concentrations (0, 80, and 640 mg/L) were referred to control, B80, and B640, respectively. We performed a pairwise comparison using 0 mg/L as the control, and B80, or B640 as the treatments. Three DEGs sequencing quality evaluations and alignment statistics are shown in Table S1. The percentage of all low-quality reads was less than 0.05% among the three libraries. In each library, 98.6% of the raw tags were clean. After filtering the low-quality tags, the total number of clean tags in each library was 3.175, 3.380, and 3.158 billion (which correspond to 98.61%, 98.60%, and 98.65% of raw tags, respectively) (Fig. S1). Among the clean tags, the numbers of sequences that could be mapped to ostrich genome sequences amounted to 15.88, 16.90, and 15.79 million respectively, which correspond to 75.68%, 76.68%, and 72.86%, respectively, in the three libraries. In the control, B80, and B640 libraries, 11.93, 12.85, and 11.41 million reads, respectively (which correspond to 75.14%, 76.04%, and 72.28%, respectively), were uniquely mapped to the ostrich genome. The number of clean reads that mapped to a gene was calculated and normalized to RPKM values to measure the extent of genes' coverage (Fig. S2). Our results showed that 72%, 71%, and 69% of the expressed genes had exhibited a sequencing coverage of 90–100% (the green portion, Fig. S2) in the control, B80, and B640 libraries, respectively.

Variation in Gene Expression Among the Three Different Groups

To identify the differentially expressed genes among the different groups, different genes between the two samples were identified according to the detection method. The libraries

produced over 3G of 100 nt double-end read data with a Q20 percentage of approximately 98%. The variations in gene expression were analyzed by comparing the control and B640, B80, and B640, and the control and B80 groups. A total of 2044 genes, including 228 upregulated and 1816 downregulated genes, were identified in the B640 group compared to the control group. There were 902 genes, of which 309 were upregulated and 593 were downregulated in the B80 group compared with the control group. The total number of differentially expressed genes was 1085, of which 222 were upregulated and 863 were downregulated between in the B80 and the B640 groups (Fig. 1).

Trend Analysis and Gene Expression Clustering

To examine the expression profiles of the 6, 260 differentially expressed genes, the expression data υ were normalized to 0, log2 (υ80/υ0), and log2 (υ640/υ0). Using Short Time-series Expression Miner software (STEM), we classified 6260 DEGs into 7 profiles, of which 3, 807 were clustered into three profiles (P value < 0.05) (Fig. 2a). Profiles 0, 1, and 3 exhibited significant clustering trends (Fig. 2b–d). Profile 0 represents genes for which the expression consistently decreased with increasing boron concentrations. Profile 1 represents the genes for which the expression initially decreased and then maintained invariably as the boron concentrations increased. Profile 3 represents genes for which expression was initially stable but then decreased. Profiles 0, 1, and 3 contained 1290, 1030, and 1487 differentially expressed genes, respectively.

GO Functional Classification Analysis of Differentially Expressed Genes

To further investigate the biological functions of differentially expressed genes, gene ontology (GO) analysis was performed to map all the DEGs (|log2 FC| > 1, P value < 0.05) to terms in the GO database. In this study, GO analysis was conducted for profiles 0, 1, and 3, all which exhibited significant trends (Fig. 1). The profiles were classified into three categories including cellular components, molecular functions, and biological processes, which were further classified into 25 functional groups. Under the biological processes category, most of the genes in profile 0 were classified into cellular, single-organism, and metabolic processes, as well as biological regulation, response to stimulus, signaling, location, multicellular organismal processes, establishment of localization, development processes, cellular component organization or biogenesis, and positive regulation of biological processes. For the molecular function category, metabolic process, catalytic activity, cellular processes, single-organism processes, biological regulation, and regulation of biological processes were the top-ranked subcategories (Fig. S3A). Genes in profiles 1 and 3 were associated with many biological processes,

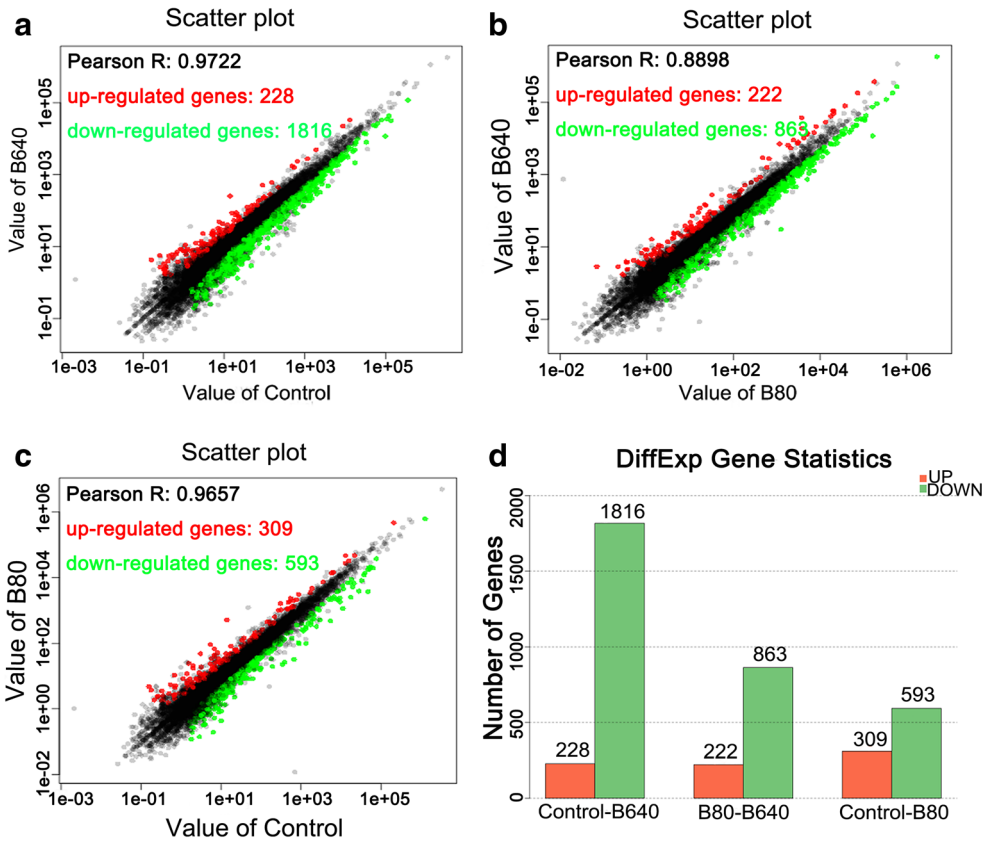

Fig. 1 Cluster analysis of different gene expression patterns. Each column represents a boron treatment (control, B80, B640: 0, 80, 640 mg/L, respectively). Scatter plot of expression differences are shown in different colors. Red and green indicate upregulated and indicate downregulated, respectively. Differentially expressed genes between the B640 and control groups (**a**), the B640 and B80 groups (**b**), the B80 and control groups (**c**), and bar-chart combining all three groups (**d**)

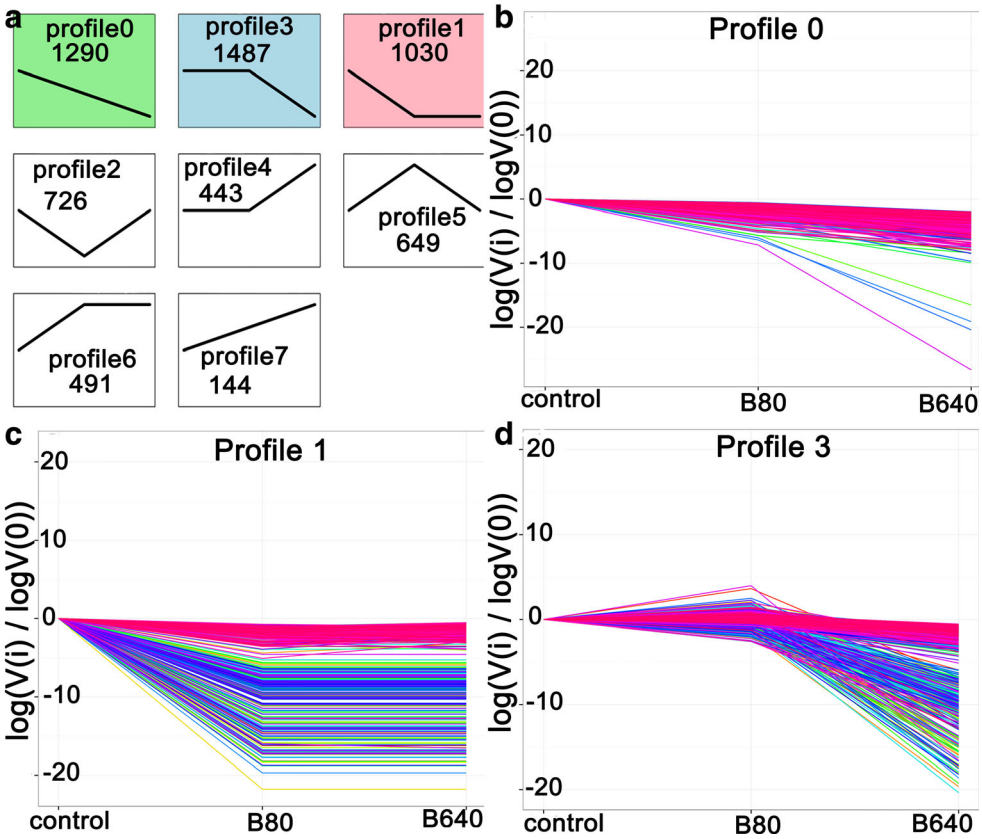

Fig. 2 Sketch map of the cluster analysis of DEGs. Filled color clusters indicate clusters with significant trends (*P* value < 0.05). DEG expression profiles (**a**). **b** Profile 0 represents genes whose expression decreases constantly with increasing boron doses. **c** Profile 1 represents genes whose expression initially decreased and then maintained invariability with increasing boron doses. **d** Profile 3 represents genes whose expression initially stable and then deceased with increasing boron doses

such as cellular, single-organism, and metabolic processes, as well as biological regulation, response to stimulus, signaling, and location. For the molecular function category, binding, metabolic processes, catalytic activity, cellular and single-organism processes, and biological regulation were the top-ranked subcategories (Fig. S3B, C). These profiles exhibited similar results in terms of their "cellular components," which included cell parts, cell, organelles, membranes, and membrane parts (Fig. S3).

KEGG Pathway Enrichment Analysis of Differentially Expressed Genes

Differentially expressed genes were subjected to KEGG pathway enrichment analysis. The top 10 KEGG pathways with the highest representation of the DEGs are shown in Table 2. The result of the KEGG enrichment analysis revealed that the main pathways associated with the differentially expressed genes were significantly enriched (*P* value < 0.05) in "metabolic pathways (ko01100)," "neuroactive ligand-receptor interaction (ko04080)," "cytokine-cytokine receptor interaction (ko04060)," "pathways in cancer (ko05200)," "calcium signaling pathway(ko04020)," "MAPK signaling pathway (ko04010)," "regulation of actin cytoskeleton (ko04810)," "focal adhesion (ko04510)," "endocytosis (ko04144)," and "purine metabolism (ko00230)."

The differentially expressed gene-associated KEGG pathways with the significant trends (profiles 0, 1, and 3) are shown in Table S2. For profile 0, the significantly enriched inflammation- and immunity-related pathways included cytokine-cytokine receptor interaction (ko04060), RIG-I-like receptor signaling pathway (ko04622), Toll-like receptor signaling pathway (ko04620), Jak-STAT signaling pathway (ko04630), apoptosis (ko04210), primary immunodeficiency (ko05340), natural killer cell-mediated cytotoxicity (ko04650), T cell receptor signaling pathway (ko04660), and NOD-like receptor signaling pathway (ko04621). For profile 3, the main pathways were significantly enriched in cytokine-cytokine receptor interaction (ko04060), adipocytokine signaling pathway (ko04920), calcium signaling pathway (ko04020), apoptosis (ko04210), and chemokine signaling pathway (ko04062), which were correlated with inflammation and immunity with statistically significant differences (*P* value < 0.05). Although there were many significant pathways for profile 1, we did not find any significant pathways correlated with immunity or inflammation.

Differentially Expressed Genes in the MAPK Signaling Transduction Pathway in Response to Boron

We also focused on the genes related to inflammation and immune response and chose specific genes involved in the

Table 2 10 top KEGG pathways with high representation of the DEGs

Pathways	No. of DEGs with pathway annotation									Pathway ID
	All profiles (% of 940)	Profile 0 (% of 276)	Profile 1 (% of 143)	Profile 2 (% of 89)	Profile 3 (% of 269)	Profile 4 (% of 36)	Profile 5 (% of 64)	Profile 6 (% of 46)	Profile 7 (% of 17)	
Metabolic pathways	194 (20.64)	57 (20.65)	30 (20.98)	15 (16.85)	48 (17.84)	6 (16.67)	16 (25.00)	16 (34.78)	6 (35.29)	ko01100
Neuroactive ligand-receptor interaction	98 (10.43)	16 (5.80)	24 (16.78)	10 (11.24)	18 (6.69)	10 (27.78)	14 (21.88)	6 (13.04)	0 (0.00)	ko04080
Cytokine-cytokine receptor interaction	64 (6.81)	21 (7.61)	7 (4.90)	5 (5.62)	21 (7.81)	1 (2.78)	4 (6.25)	4 (8.70)	1 (5.88)	ko04060
Pathways in cancer	57 (6.06)	17 (6.16)	10 (6.99)	9 (10.11)	11 (4.09)	3 (8.33)	2 (3.12)	5 (10.87)	0 (0.00)	ko05200
Calcium signaling pathway	52 (5.53)	13 (4.71)	8 (5.59)	5 (5.62)	17 (6.32)	4 (11.11)	2 (3.12)	3 (6.52)	0 (0.00)	ko04020
MAPK signaling pathway	50 (5.32)	16 (5.80)	5 (3.50)	6 (6.74)	16 (5.95)	1 (2.78)	1 (1.56)	2 (4.35)	3 (17.65)	ko04010
Regulation of actin cytoskeleton	47 (5.00)	14 (5.07)	6 (4.20)	5 (5.62)	15 (5.58)	1 (2.78)	2 (3.12)	4 (8.70)	0 (0.00)	ko04810
Focal adhesion	41 (4.36)	13 (4.71)	5 (3.50)	6 (6.74)	13 (4.83)	2 (5.56)	1 (1.56)	1 (2.17)	0 (0.00)	ko04510
Endocytosis	40 (4.26)	16 (5.80)	1 (0.70)	2 (2.25)	14 (5.20)	1 (2.78)	0 (0.00)	2 (4.35)	4 (23.53)	ko04144
Purine metabolism	36 (3.83)	11 (3.99)	4 (2.80)	5 (5.62)	8 (2.97)	1 (2.78)	5 (7.81)	1 (2.17)	1 (5.88)	ko00230

MAPK signaling pathway that exhibited significantly different expression among the three groups (Figs. 3 and 4). The heat map diagram showed that most genes of the MAPK pathways were downregulated in the B640 group compared with the control group. In the B80 group, the expression of specific genes was increased, whereas others remained unchanged compared to the control group. In the MAPK signaling pathway, 24 out of the 27 DEGs exhibited downregulated trends, of which 3 exhibited upregulated trends in the B640 group, indicating that high-dose boron (640 mg/L) could downregulate the MAPK signaling pathway in the ostrich thymus. Simultaneously, 22 out of the 27 DEGs exhibited upregulated or unchanged expression trends, of which 5 exhibited downregulated trends in the B80 group, indicating that low-dose boron (80 mg/L) can also regulate the MAPK signaling pathway in the ostrich thymus. The MAPK signaling pathways generally comprises extracellular signal-related kinases (ERK1/2), Jun amino-terminal kinases (JNK1/2/3), p38 proteins, and the ERK5 signaling pathway. In the classical MAPK pathway, also known as the Ras/ERK pathway, boron predominantly regulated the Sca_R002724 (FGF), Sca_R004594 (EGFR), Sca_R011737 (Gap1m), Sca_R007189 (Ras), Sca_R010278 (PKA), Sca_R009322 (Rap1), Sca_R006605 (MP1), Sca_R004261 (ERK), and Sca_R005585 (RSK2) genes involved in the signaling pathway. In the JNK pathway, boron predominantly regulated the Sca_R007279 (MEKK1), Sca_R014908 (JNK), Sca_R012401 (JIP1/2), Sca_R011070 (Evil), Sca_R001662, Sca_R007824 (HSP72), Sca_R008551 (PPP3CA), Sca_R006610 (PPP3R1), and Sca_R002897 (NFAT-2) genes. In the p38MAPK signaling pathway, boron predominantly regulated the Sca_R007425 (IL-1R), Sca_R011264 (p38), Sca_R002488 (MKP), Sca_R004878 (MEF2C), and Sca_R006958 (MSK1/2) genes. However, we did not observe any genes that were differentially expressed in the ERK5 signaling pathway.

Real-Time Quantitative RT-PCR Validation of DEG Analysis

Twenty genes were examined for their expression levels using qRT-PCR to validate the conclusions drawn from the RNA-Seq data; all the examined genes behaved as predicted (Fig. 5). The results revealed differential expression among the six groups and were identical to those obtained by DGE expression profiling (control, B80, B640). Real-time quantitative PCR analysis suggested that genes involved in the inflammation, immune response, and growth factor activity comprised a network of interactions, providing the mechanism of action of boron affecting the immune response of ostrich chicks. Thus, the data generated in this study were sufficient for investigating the mechanism of action of boron affecting immune response, which revealed comparative expression levels among different boron concentrations.

Expression Levels of the Candidate Genes in Response to Different Doses of Boron

Based on KEGG pathway enrichment analysis, most of the genes associated with calcium, cancer, and MAPK signaling

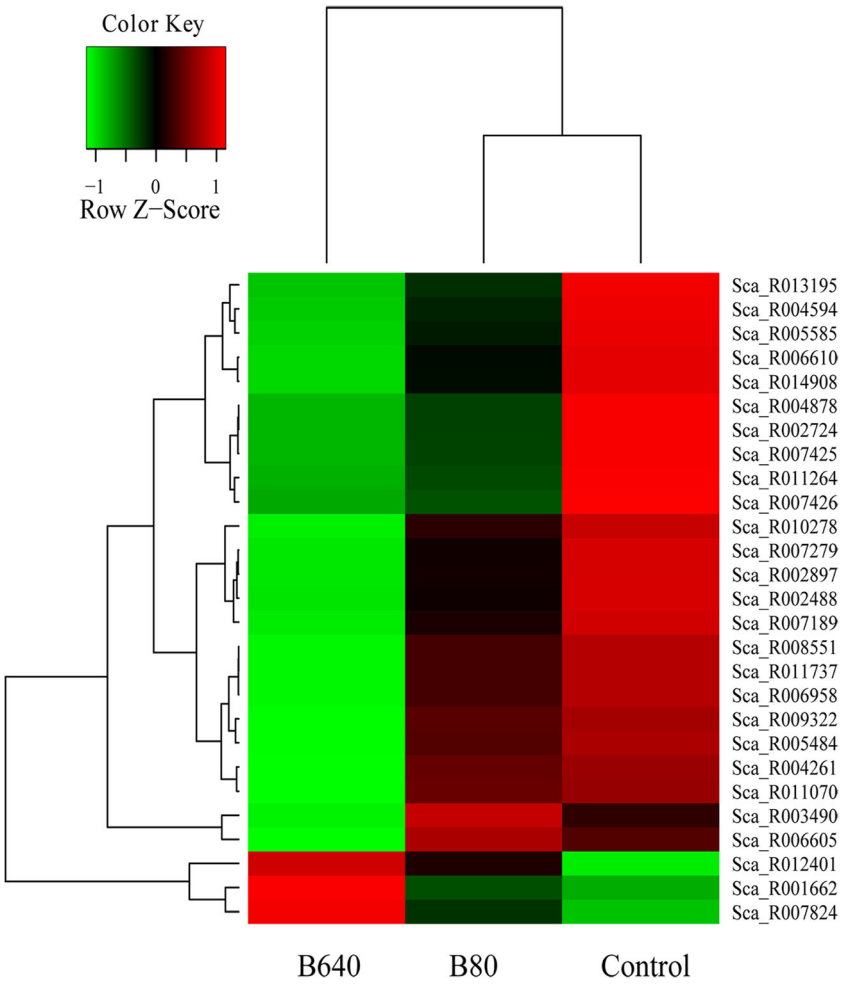

Fig. 3 Heat map diagram of differential expression in MAPK signaling pathway analyzed by KEGG. Each column represents an experimental sample (e.g., control, B80, and B640), and each row represents a gene. Expression differences are shown in different colors. Red indicates high expression, whereas green indicates low expression

pathways were induced by boron. We selected 20 candidate genes and analyzed their expression levels during treatment with a gradient of boric acid (0, 40, 80, 160, 320, and 640 mg/L). We also checked 8 candidate proteins and analyzed their expression among the different boric acid groups.

The calcium signaling pathway is predominantly involved in cell survival/-apoptosis, cell cycle progression, and differentiation. The crucial role of the calcineurin/NFAT signaling pathway in T cell downstream activation of TCR engagement is responsible for the initiation of a productive immune response [41]. The calcineurin complex is composed of a catalytic subunit A (CnA) and a regulatory subunit B (CnB). CnA and CnB are crucial for calcineurin activity. Thus, we assessed the expression of PPP3CA (CnA) and PPP3R1 (CnB) in this study (Figs. 5a, b and 6g, h). The qRT-PCR results revealed that the expression trends of the PPP3CA and PPP3R1 were both initially increased at the lower dosage of boron and then decreased after the peak at the higher doses of boron. In addition, boron predominantly regulates the expression of PPP3R1 in ostrich thymus. Eighty milligrams per liter of boric acid significantly upregulated the mRNA levels of PPP3R1, up to 26 times that of the control group (Fig. 5b). Although the mRNA levels of PPP3CA were lower than those of the PPP3R1, 80 mg/L of boric acid also significantly increased the mRNA levels of PPP3CA. However, 640 mg/L boric acid could downregulate the mRNA level of PPP3CA compared with the control group (Fig. 5a). The protein expression levels of PPP3CA and PPP3R1 in the ostrich thymus exhibited a similar trend, and the results were consistent with the qRT-PCR results (Fig. 6g, h). Activation of NFAT proteins follows precisely the activation pattern of calcineurin. According to our DEG results, the expression of NFAT-2 in the ostrich thymus was detectable (Fig. 5c). The results revealed that the mRNA levels of NFAT-2 in the ostrich thymus initially increased and declined sharply with increasing boron dosage. The mRNA levels of NFAT-2 peaked in the 80 mg/L of boric acid group, whereas they significantly reduced in the 640 mg/L of boric acid.

We demonstrated that both mRNA and protein expression levels of ERK, JNK, and p38 were significantly increased in the 80 mg/L of boric acid group (Figs. 5f–h and 6b, d, f). The mRNA levels of ERK and JNK increased 18.3-fold and 15.7-fold in 80 mg/L respectively, in the 80 mg/L of boric acid group, whereas the mRNA levels of p38 only increased

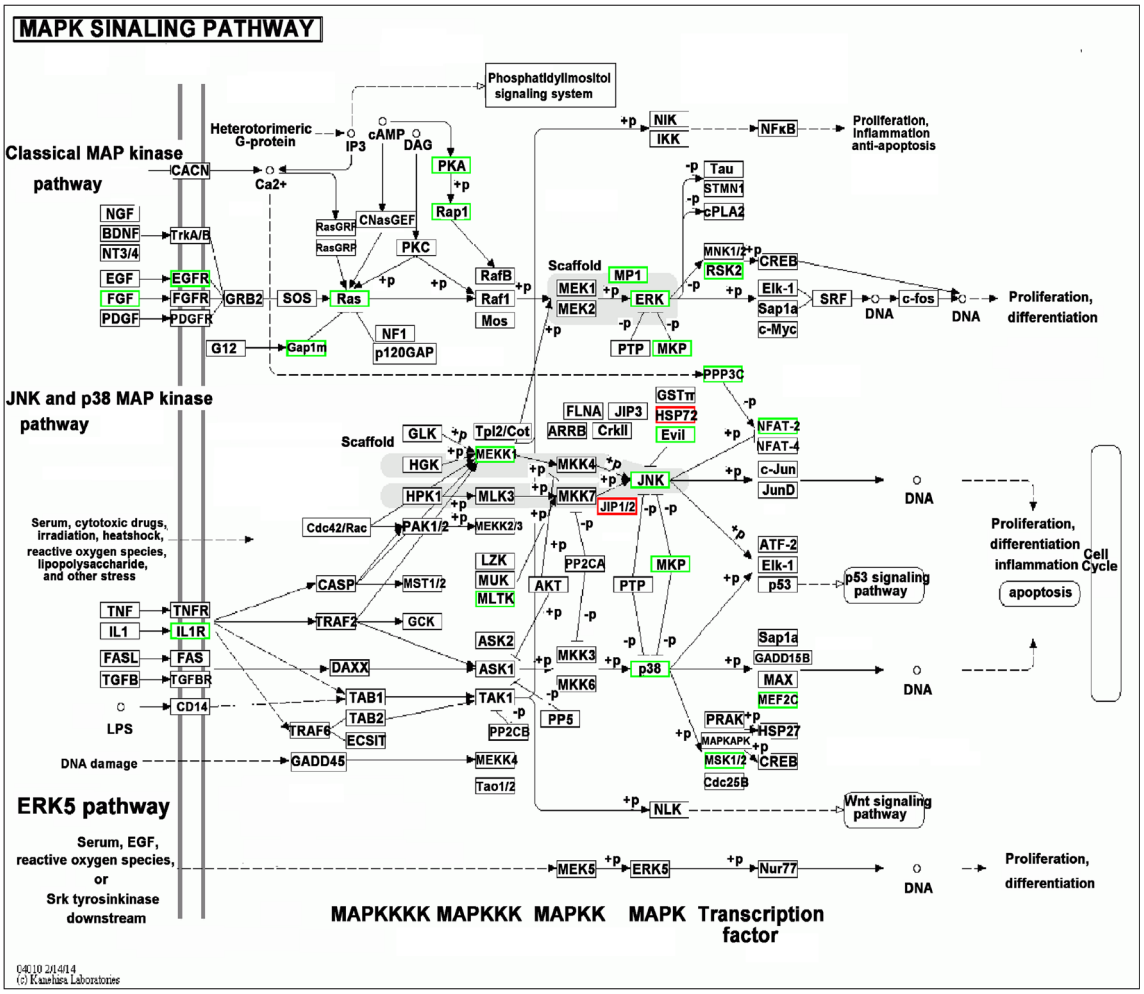

Fig. 4 MAPK signaling transduction pathway. The components marked with rectangles indicate differentially expressed genes. The green rectangle repesents the downregulated genes, and the red rectangle represents the upregulated genes

moderately 2- to 3-fold in the 80 mg/L of boric acid group. As shown in Fig. 4, the mRNA levels of the MAPK signaling pathway genes gradually increased and then decreased in a boron dose-dependent manner. The effects of boron on the activation of extracellular signal-regulated kinase (ERK), C-Jun N-terminal kinase (JNK), and p38 were also confirmed at the protein level by Western blot analysis (Fig. 6). The ostrich thymuses in the 80 mg/L of boric acid group exhibited increased expression levels of p-ERK, p-JNK, and p-p38 compared with the control group. The expression levels of p-ERK, p-JNK, and p-p38 was gradually attenuated in a boron dose-dependent manner after 80 mg/L, reaching the lowest levels at 640 mg/L. These results suggested that the immune response to boron is mediated by the MAPK signaling pathway in the ostrich thymus.

The activity of the Ras/ERK pathway is required for cell survival and normal growth. The results presented in Fig. 5 show that 80 mg/L of boric acid significantly elevated the mRNA level s of the ERK compared with the control group, whereas higher dosages of boron reduced the mRNA levels of ERK. Although the mRNA levels of the ERK were increased in the high-dose boron group (640 mg/L), the protein expression levels of p-ERK (42kd, 44kd) were reduced in the high-dose boron group compared to that observed in the control group (Fig. 6a, b).

The JNK signaling pathway plays a crucial role in T cell differentiation and cytokine production. The results presented in Figs. 5 and 6 demonstrate that the expression levels of JNK and p-JNK are the same as that of ERK and p-ERK. Boron induced the expression of JNK and ERK at the same time. Our data indicate that boron predominantly regulates the expression levels of ERK and JNK but not p38.

Discussion

Boron is essential for growth and is known to play an important role in immune response [6]. Boron deficiency has been

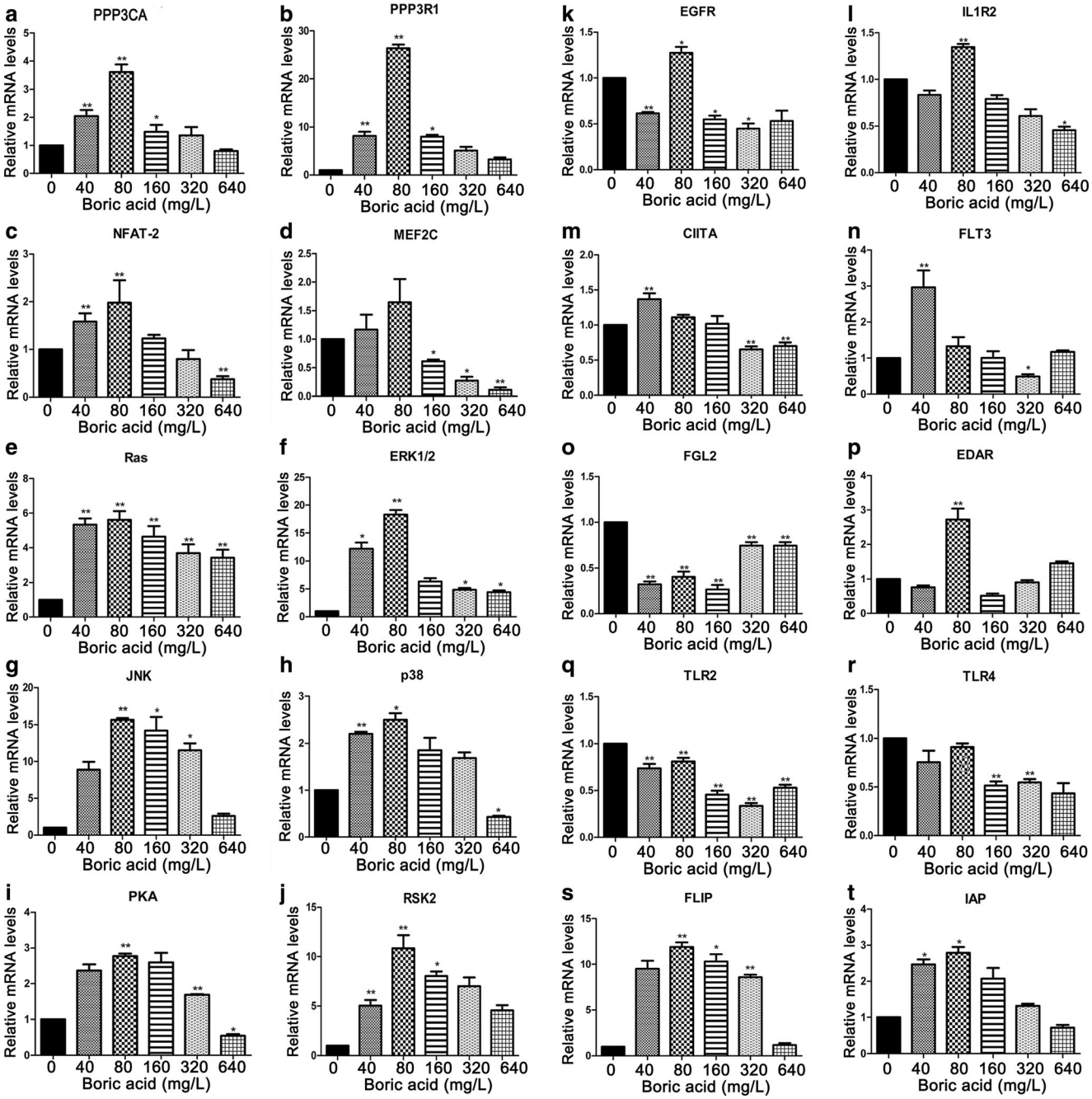

Fig. 5 Real-time quantitative PCR results of differentially expressed genes in different boric acid groups. Data from the real-time quantitative PCR are mean values of three biological replicates. **a** PPP3CA. **b** PPP3R1. **c** NFAT-2. **d** MEF2C. **e** Ras. **f** ERK1/2. **g** JNK. **h** P38. **i** PKA. **j** RSK2. **k** EGFR. **l** IL1R2. **m** CIITA. **n** FLT3. **o** FGL2. **p** EDAR. **q** TLR2. **r** TLR4. **s** FLIP. **t** IAP

related with poor immune function, increased risk of mortality, whereas its toxic level passed on injury to cells and toxicity in animals and humans. Experimental animals have shown pronounced signs of enhanced immunity following administration of boron. When rats were offered with two different levels of boron supplementation with low boron diet (0.2 mg/kg) and high boron diet (3 mg/kg), enhancement in immune response was seen in the low boron diet group [42], evident from the study of Hu et al. demonstrated that 40 mg/L boron could increase body weight, organ indexes, and antioxidant capacity of spleen and improve the spleen tissue structure, and low boron supplementation played a protective role in the spleen development, whereas high boron supplementation damaged the rat organs and even produced toxic effect [43]. In an another study, it was reported that laying hens from 26 to 42 weeks of age should be fed with 60 mg/kg boron and 150 mg/kg copper supplementation in the diet [44]. An appropriate boron level supplementation can promote thymus

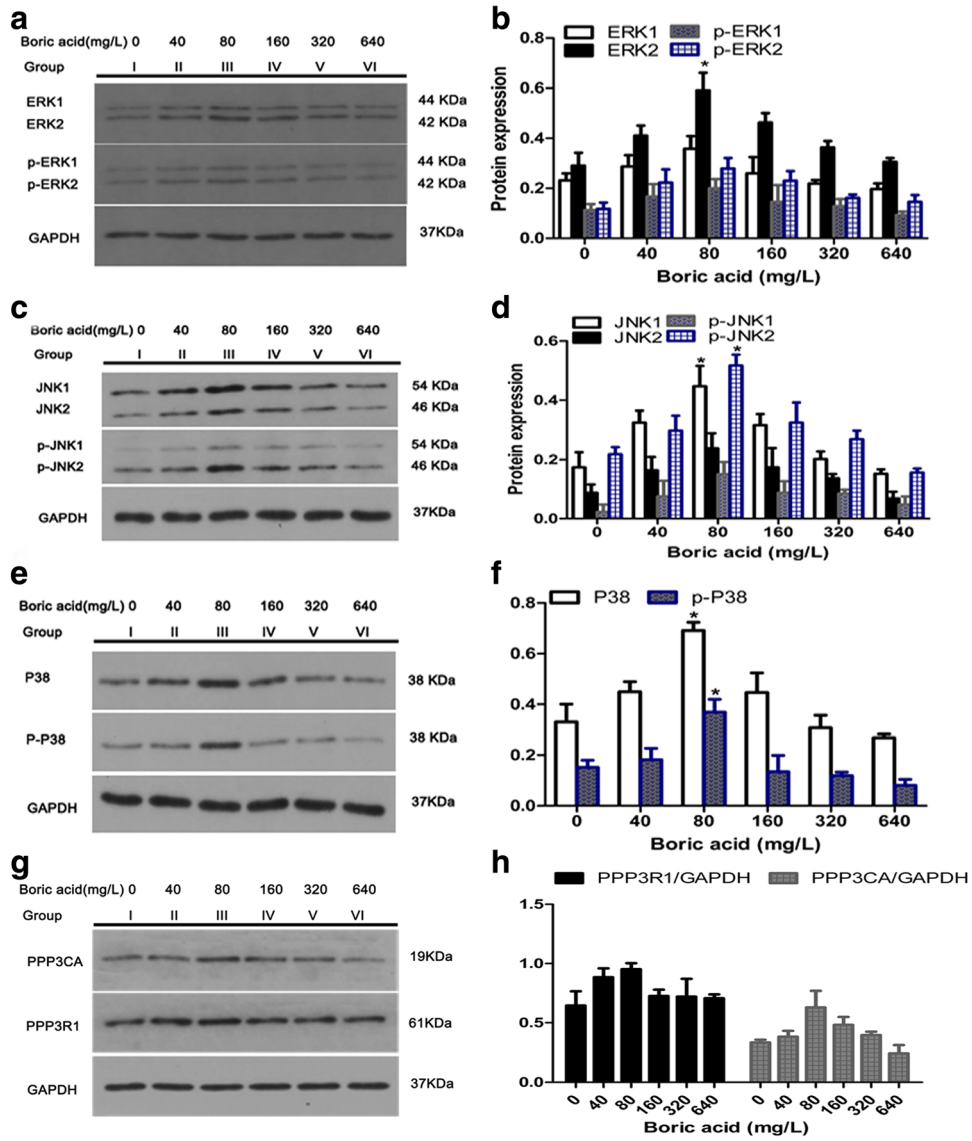

Fig. 6 Boron induces the expression of ERK1/2, p-ERK1/2, JNK1/2, p-JNK1/2, p38, p-p38, PPP3CA, and PPP3R1. The bar graphs and representative Western blots show that boron induces the expression of ERK1/2, p-ERK1/2 (**a**, **b**), JNK1/2, p-JNK1/2 (**c**, **d**), p38, p-p38 (**e**, **f**), PPP3CA, and PPP3R1 (**g**, **h**). The representative results and densitometric analyses from at least three independent experiments are shown. $^{*}P < 0.05$ vs. control

development in rats, as well as enhance cellular immune function and attract more natural killer (NK) cells [45]. Furthermore, appropriate supplements of boron (< 100 mg/L) could improve the growth of immune organs in broilers after 4 weeks [9]. Our previous studies have also demonstrated that boron can regulate the immune response in ostriches [10]. Ostrich chicks supplemented with 80–160 mg/L of boron exhibited a positive effect on the final body weight [37]. Appropriate dosage of boron supplementation can improve ostrich chick growth performance by upregulating BW, ADFI, and ADG, whereas high-dose boron supplementation can inhibit growth performance [37]. Thymus mediates cellular immunity and supports the maturation of T lymphocytes, and low-dose boron supplementation promotes the Foxn1 expression and facilitates the ostrich chick thymus development; however, high-dose boron supplementation can damage ostrich thymus structure and suppress the immune function [10]. After high-dose boron supplementation, the amount of apoptotic thymic cells tends to increase, and the expression of autophagy and proliferation markers (ssDNA, LC3A/B, PCNA) increase significantly in ostrich chick thymuses [47]. However, little is known about the mechanisms underlying the boron-induced immune response of ostriches. This is the first study to generate a significant amount of cDNA sequence data that can facilitate further detailed studies about the mechanism of action of boron and identify the genes that boron-induced immune response. The availability of transcriptomic data for different doses of boron will provide the initial information necessary for mechanistic studies of boron in the ostrich thymus. Twenty of the differentially expressed genes identified by RNA-seq were validated by qRT-PCR. Although the differences in gene expression based on qRT-PCR did not match the magnitude of those detected

using RNA-seq, the upregulation and downregulation trends were similar, indicating a desirable quality of transcriptomic data.

In our present study, we found that boron is closely related with cancer pathways. In agreement with our findings, boron revealed the actions as an anti-inflammatory and antioxidant agent in cancer, modulating mitochondrial membrane activity, wound healing, and disease control [9, 42, 45]. Thus, boron is very useful to overcome breast cancer cells in vitro, and the cancer therapy can be ensured by boron capture agents. Furthermore, the experimental and epidemiological studies have demonstrated that boron has a positive effect on human prostate cancer cells, and the anti-cancerous effects of boron may be associated with its action on NAD and calcium channel. Boron inhibited the proliferation of tumor cell lines PC-3, DU-145, and LNCaP in a dose-dependent manner and had a good inhibitory effect on tumor cell growth [46, 54]. When boron was added to the diet of the immune system damaged mice, the human prostate cancer tumor that was transplanted into the mice showed a downtrend. It was also observed that dietary boron can reduce the risk of breast cancer and lung cancer in women [42]. In conclusion, according to our findings in the present study and the previous findings, boron agents have an important role in cancer treatment.

The calcium/calcineurin/NFAT signaling pathway was initially identified in mature T cells and is important at specific stages of their biology (pre-TCR signaling, TCR-mediated positive selection) during thymocyte development [48]. In this study, boron predominantly regulates the expression of PPP3R1 to control calcineurin activity. PPP3R1 is the regulatory subunit B of the calcineurin. Low-dose boron (80 mg/L) promoted the expression of PPP3CA and PPP3R1, whereas high-dose boron (640 mg/L) downregulated or inhibited the expression of PPP3CA and PPP3R1 in the ostrich thymus. Previous studies have demonstrated that a high dose of boron (400 mg/L) significantly inhibited lymphocytes multiplication in Gushi Chick, and in parallel, the concentration of both calcium and magnesium ions remarkably decreased in the blood [49]. In addition, Goihl et al. demonstrated that low level of boron supplementation to the swine feed was favorable, causing better weight gain, feed efficiency, and calcium maintenance in the body [50]. Prolonged increases in calcium ion levels were required in T cells to maintain calcineurin and NFAT proteins in an activated state [51]. The results from this study demonstrated that high-dose boron (640 mg/L boric acid) inhibits calcineurin activity by downregulating the mRNA levels of PPP3CA and PPP3R1 in the ostrich thymus, which might be attributed to the decreased calcium levels associated with high-dose boron treatment. Consequently, low levels of calcium ions would be insufficient for T cells to maintain an activated state of the calcineurin and NFAT proteins. At the same time, a boron deficiency might upset the intrinsic plasma concentration balance between calcium, magnesium, and phosphorus [7]. Eighty milligrams per liter of boric acid promoted calcineurin activity to participate in thymocyte development and immune responses in the ostrich thymus [10, 47]. As a consequence, an appropriate dose of boron is necessary for the health of body. The activity of NFAT proteins is tightly regulated by the calcium/calmodulin-dependent phosphatase calcineurin. NFAT proteins are expressed in the lymphoid lineage, and their best characterized function is their crucial involvement in the development, differentiation, and function of multiple T/B cell subsets [53]. In this study, 80 mg/L of boric acid significantly upregulated the protein expression levels of NFAT-2, whereas 640 mg/L of boric acid significantly inhibited its expression. These results suggest that high-dose boron inhibit T cells activation by inhibiting thymocyte development, T cell differentiation, and self-tolerance by inhibiting NFAT proteins [53]. On the other hand, appropriate doses of boron (80 mg/L of boric acid) can promote thymocyte development. Barranco et al. reported that the anti-carcinogenic effects of boron may be associated with its action on NAD and calcium channel. Boron causes a dose-dependent decrease of Ca^{2+} release from ryanodine receptor-sensitive stores [46]. In addition, boric acid inhibits NAD^{+} and $NADP^{+}$ as well as mechanically induced release of stored Ca^{2+} in growing DU-145 prostate cancer cells [54]. It was suggested that boric acid binds to a site on the ryanodine receptor so that it can keep Ca^{2+} channel inactive in the cancer lines [42]. These reports are consistent with our findings, 640 mg/L boric acid significantly inhibited the calcium pathway, maybe the toxicity of boric acid stems from the ability of high concentrations to impair Ca^{2+} signaling [54]. In short, boron can regulate ostrich thymus development and induce immune responses by regulating the calcium signaling pathways, particularly the calcineurin/NFAT signaling pathway. In addition, the toxic mechanism of high concentration boric acid originates from the ability to impair calcium pathway.

The MAPK signaling pathway is an evolutionarily conserved signaling pathway, which is important for many processes in immune responses from the innate to the adaptive immune system and from the initiation of immune responses to the activation-induced cell apoptosis [20]. The ERK pathway was the first identified downstream of Ras and is involved in the regulation of cell growth and differentiation. The Ras-ERK transduction pathway is required for immature thymocyte differentiation from the DN to the DP stage, positive selection of T cells, and T cell lineage commitment [28]. ERK activation is important for T cell activation. In this study, ERK was expressed in a boron dose-dependent manner. Low-dose boron (80 mg/L of boric acid) significantly increased the expression levels of ERK and p-ERK, which might be associated with the activated body protection mechanisms in ostriches. When the boron dosage was increased, the expression levels of ERK and p-ERK were decreased. It is likely that a high dose of boron damages thymocytes and induces apoptosis in the ostrich thymus [10], retards normal cell growth and

differentiation in the thymus, inhibits body protection mechanisms, and leads to reduced expression levels of ERK in the thymus. There is a strong consensus on the role of the ERK pathway in thymocyte selection. Other studies have shown that ERK1-deficient mice exhibit defective thymocyte maturation [52]. Taken together, these data suggest that boron is involved in the thymocyte selection by regulating ERK kinase activity.

JNK activity in the cell is tightly controlled by both protein kinases and protein phosphatases [23]. In this study, the expression patterns of JNK and p-JNK were the same as those of ERK and p-ERK. In terms of the MAPK signaling pathway, boron predominantly regulates the ERK and JNK signaling pathways. Furthermore, it is worth noting that in this study, low-dose boron significantly and simultaneously increased the mRNA levels of ERK and JNK. Specifically, JNK signaling has been reported to be pro-apoptotic [23], and JNK can reduce the proliferative responses of the activated T cells and regulate apoptosis in T cells [18]. To restrict excessive inflammation, the number of activated lymphocytes in the body is tightly regulated. The MAPK signaling pathway is important for the regulation of cellular survival and apoptosis in lymphocytes. We therefore speculate that JNK might be antagonized by ERK in the ostrich thymus. Activation of ERK promoted T cells activation in the thymus in the low-dose boron group (80 mg/L). In order to prevent excessive T cell activation, the expression levels of JNK were upregulated significantly in ostrich thymuses in the low-dose boron group (80 mg/L), thus maintaining T cell activation at a normal level.

In this study, a low-dose boron (80 mg/L) elevated the expression of p38 and p-p38 in the ostrich thymus, indicating that p38 MAP kinase activity was increased in the 80 mg/L of boric acid group. Following the activation of p38 MAP kinase, early T cell development is triggered in the thymus [18, 27]. Previous reports indicate that p38 MAPK can modulate and increase the expression of several transcription factors (e.g., myocyte enhancer factor 2C (MEF 2C) [53]. This might explain why the expression levels of MEF 2C in this study were the same as those of p38 MAP kinase. Furthermore, the p38 signaling pathway plays significant roles in many cellular processes and responses in T and B cells, and the function of p38 in regulating gene expression is important in adaptive immunity [27]. Other studies have shown that regulation of the p38 MAP kinase pathway in T cells is essential for the maintenance of CD4/CD8 homeostasis in the peripheral immune system [53]. We therefore speculate that a low dose of boron (80 mg/L) can improve adaptive immunity by regulating p38 MAP kinase activity. Conversely, a high dose of boron (640 mg/L) inhibits p38 expression, specifically, p38 MAP kinase activity. The inhibition of p38 MAP kinase causes defects in early thymocyte development [21].

Barranco et al. showed that boron caused a dose-dependent reduction in MAPK protein and cyclins A-E, showing the contribution to proliferative inhibition in DU-145 prostate cancer cells. Previous studies also demonstrated that the effect of boric acid on growth and cell proliferation in zebrafish, trout, and the mammalian Hela and Hek cells follows an inverted U shape with higher concentrations causing cell growth inhibition [42, 54]. In addition, our previous study found that a high dose of boron results in induced the reduced and exhausted lymphocytes in the ostrich's thymus [10]. These data demonstrated that a high-dose of boron inhibits early T cells development and proliferation in ostrich thymus by downregulating MAP kinase activity, which attenuates adaptive immunity in the ostrich.

Conclusion

RNA-Seq analysis based on Illumina sequencing technology provided comprehensive gene expression information of the ostrich thymus. These data represent useful tools for the investigation of the mechanisms underlying the functional roles of boron in the ostrich immune system. In addition, the calcium and MAPK signaling pathways might play a crucial role in the regulation of the immune responses of the ostriches treated with boron.

Funding information This study was supported by the National Natural Science Foundation Projects of China (No. 31672504), the National Natural Youth Science Foundation of China (No. 31702196), and the National Science Foundation for Post-doctoral Scientists of China (No. 2017M612482).

Compliance with Ethical Standards

The present study was approved by the Ethics Committee of Huazhong Agricultural University. Protocols of animals were performed according to the No. 5 Proclamation of the standing Committee of Hubei People's Congress, People's Republic of China.

Conflict of Interest The authors declare that they have no competing interest.

Abbreviations RNA-seq, Illumina RNA sequencing; DEGs, differentially expressed genes; GO, gene ontology; KEGG, Kyoto Encyclopedia of Genes and Genomes; B80, 80 mg/L boric acid; B640, 640 mg/L boric acid; qRT-PCR, quantitative reverse transcription PCR; MAP, mitogen-activated protein kinase; ERK1/2, extracellular signal-related kinase; p-ERK1/2, phospho-extracellular signal-related kinase; JNK1/2, Jun amino-terminal kinases; p-JNK1/2, phospho-Jun amino-terminal kinase; p38MAPK, p38 mitogen-activated protein kinase; p-p38MAPK, phospho-p38 mitogen-activated protein kinase; PPP3CA, protein phosphatase 3, catalytic subunit, alpha isozyme; PPP3R1, protein phosphatase 2B regulatory subunit 1; NFAT-2, nuclear factor of activated T cells; MEF2C, myocyte enhancer factor 2C; PVDF, polyvinylidene fluoride membranes

References

1. Johnston P (2011) New morphological evidence supports congruent phylogenies and Gondwana vicariance for palaeognathous birds. Zool J Linn Soc-Lond 163(3):959–982
2. Mitchell KJ, Llamas B, Soubrier J, Rawlence NJ, Worthy TH, Wood J (2014) Ancient DNA reveals elephant birds and kiwi are sister taxa and clarifies ratite bird evolution. Science 344(6186): 898–900
3. Alnasser A, Alkhalaifa H, Holleman K, Al-Ghalaf W (2003) Ostrich production in the arid environment of Kuwait. J Arid Environ 54(1):219–224
4. Bejaei M, Cheng KM (2014) A survey of current ostrich handling and transport practices in North America with reference to ostrich welfare and transportation guidelines set up in other countries. Poultry Sci 93(2):296–306
5. Pittaway T, Niekerk PV (2015) Horizon-scanning the ostrich industry with bibliometric indicators. AfJARE 10:64–71
6. Bonato M, Evans MR, Hasselquist D, Sherley RB, Cloete SWP, Cherry MI (2013) Ostrich chick humoral immune responses and growth rate are predicted by parental immune responses and paternal colouration. Behav Ecol Sociobiol 67(12):1891–1901
7. Kabu M, Akosman MS (2013) Biological effects of boron. Reviews of environmental contamination and toxicology. Springer, New York, pp 57–75
8. Kabu M, Civelek T (2012) Effects of propylene glycol, methionine and sodium borate on metabolic profile in dairy cattle during periparturient period. Rev Med Vet-Toulouse 163(8):419–430
9. Jin E, Gu Y, Wang J, Jin G, Li S (2014) Effect of supplementation of drinking water with different levels of boron on performance and immune organ parameters of broilers. Ital J Anim Sci 13(2):124
10. Xiao K, Ansari AR, Rehman Z, Khaliq H, Song H, Tang J, Wang J, Wang W, Sun PP, Zhong J, Peng KM (2015) Effect of boric acid supplementation of ostrich water on the expression of Foxn1 in thymus. Histol Histopathol 30(11):1367–1378
11. Jing W, Zhong JM, Sun PP, Ke X, Tang J, Wei W, Peng KM (2015) Effect of boron administration on the morphology of ostrich chick kidney tissue. Pak Vet J 35(4):489–493
12. Cheng J, Peng KM, Jin E, Zhang Y, Liu Y, Zhang N (2011) Effect of additional boron on tibias of African ostrich chicks. Biol Trace Elem Res 144(1–3):538–549
13. Sun PP, Luo Y, Wu XT, Ansari AR, Wang J, Yang KL, Zhong JM, Peng KM (2016) Effects of supplemental boron on intestinal proliferation and apoptosis in African ostrich chicks. Int J Morphol 34(3):830–835
14. Tang J, Zheng XT, Xiao K, Wang KL, Wang J, Wang YX, Zhong JM, Peng KM (2016) Effect of boric acid supplementation on the expression of BDNF in African ostrich chick brain. Biol Trace Elem Res 170(1):1–8
15. Haseeb K, Wang J, Xiao K, Yang KL, Sun PP, Wu XT, Zhong JM, Peng KM (2017) Effects of boron supplementation on expression of Hsp70 in the spleen of African ostrich. Biol Trace Elem Res 182(4): 1–11
16. Krishna M, Narang H (2008) The complexity of mitogen-activated protein kinases (MAPKs) made simple. Cell Mol Life Sci 65(22): 3525–3544
17. Bubici C, Papa S (2014) JNK signalling in cancer: in need of new, smarter therapeutic targets. Brit J Pharmacol 171(1):24–37
18. Huang G, Shi LZ, Chi H (2009) Regulation of jnk and p38 MAPK in the immune system: signal integration, propagation and termination. Cytokine 48(3):161–169
19. Kaminska B (2005) MAPK signalling pathways as molecular targets for anti-inflammatory therapy from molecular mechanisms to therapeutic benefits. BBA-Proteins Proteom 1754(1–2):253–262
20. Bedognetti D, Roelands J, Decock J, Wang E, Hendrickx W (2017) The MAPK hypothesis: immune-regulatory effects of MAPK-pathway genetic dysregulations and implications for breast cancer immunotherapy 1(5): 429–445
21. Hsu SC, Wu CC, Han J, Lai MZ (2003) Involvement of p38 mitogen-activated protein kinase in different stages of thymocyte development. Blood 101(3):970–976
22. Crompton T, Gilmour KC, Owen MJ (1996) The MAP kinase pathway controls differentiation from double-negative to double-positive thymocyte. Cell 86(2):243–251
23. Tournier C (2013) The 2 faces of JNK signaling in cancer. Genes Cancer 4(9–10):397–400
24. Hamdi M, Kool J, Cornelissen-Steijger P, Carlotti F, Popeijus HE, van der Burgt C, Janssen JM, Yasui A, Hoeben RC (2005) DNA damage in transcribed genes induces apoptosis via the JNK pathway and the JNK-phosphatase MKP-1. Oncogene 24(48):7135–7144
25. Kyriakis JM, Avruch J (2001) Mammalian mitogen-activated protein kinase signal transduction pathways activated by stress and inflammation. Physiol Rev 81(2):807–869
26. Roux PP, Blenis J (2004) ERK and p38 MAPK-activated protein kinases: a family of protein kinases with diverse biological functions. Microbiol Mol Biol Rev 68(2):320–344
27. Cook R, Wu CC, Kang YJ, Han J (2006) The role of the p38 pathway in adaptive immunity. Cell Mol Immunol 4:253–259
28. Dodeller F, Schulze-Koops H (2006) The p38 mitogen-activated protein kinase signaling cascade in CD4 T cells. Arthritis Res Ther 8:205
29. Zhang JX, Wu KL, Zeng SJ, da Silva JAT, Zhao XL, Tian CE, Xia HQ, Duan J (2013) Transcriptome analysis of cymbidium sinense and its application to the identification of genes associated with floral development. BMC Genomics 14(1):279
30. Mortazavi A, Williams BA, McCue K, Schaeffer L, Wold B (2008) Mapping and quantifying mammalian transcriptomes by RNA-Seq. Nat Methods 5:621–628
31. Wang Z, Gerstein M, Snyder M (2009) RNA-Seq: a revolutionary tool for transcriptomics. Nat Rev Genet 10:57–63
32. Polato NR, Vera JC, Baums IB (2011) Gene discovery in the threatened elkhorn coral: 454 sequencing of the Acropora palmata transcriptome. PLoS One 6(12):e28634
33. Wan L, Han J, Sang M, Li A, Wu H, Yin S, Zhang C (2012) De novo transcriptomic analysis of an oleaginous microalga: pathway description and gene discovery for production of next-generation biofuels. PLoS One 7(6):e35142
34. Lu X, Kim H, Zhong S, Chen H, Hu Z, Zhou B (2014) De novo transcriptome assembly for rudimentary leaves in litchi chinesis sonn and identification of differentially expressed genes in response to reactive oxygen species. BMC Genomics 15(1):805
35. Zhao X, Mo D, Li A, Gong W, Xiao S, Zhang Y, Qiu L, Guo Y, Liu X, Cong P, He Z, Wang C, Li J, Chen Y (2011) Comparative analyses by sequencing of transcriptomes during skeletal muscle development between pig breeds differing in muscle growth rate and fatness. PLoS One 6(5):e19774
36. Yang C, Jiang M, Wen H, Tian J, Liu W, Wu F, Guo G (2015) Analysis of differential gene expression under low-temperature stress in Nile tilapia (oreochromis niloticus) using digital gene expression. Gene 564(2):134–140
37. Wang W, Xiao K, Zheng X, Zhu D, Yang Z, Tang J, Sun P, Wang J, Peng KM (2014) Effects of supplemental boron on growth performance and meat quality in African ostrich chicks. J Agric Food Chem 62(46):11024–11029
38. Audic S, Claverie JM (1997) The significance of digital gene expression profiles. Genome Res 7(10):986–995
39. Ernst J, Bar-Joseph Z (2006) Stem: a tool for the analysis of short time series gene expression data. BMC Bioinformatics 7(1):191

40. Kanehisa M, Araki M, Goto S, Hattori M, Hirakawa M, Itoh M, Katayama T, Kawashima S, Okuda S, Tokimatsu T, Yamanishi Y (2008) KEGG for linking genomes to life and the environment. Nucleic Acids Res 36:480–484
41. Monticelli S, Rao A (2002) NFAT1 and NFAT2 are positive regulators of IL-4 gene transcription. Eur J Immunol 32(10):2971–2978
42. Khaliq H, Juming Z, Kemei P (2018) The physiological role of boron on health. Biol Trace Elem Res 2:1–21
43. Hu Q, Li S, Qiao E, Tang Z, Jin E, Jin G et al (2014) Effects of boron on structure and antioxidative activities of spleen in rats. Biol Trace Elem Res 158(1):73–80
44. Olgun O, Yazgan O, Cufadar Y (2013) Effect of supplementation of different boron and copper levels to layer diets on performance, egg yolk and plasma cholesterol. J Trace Elem Med Biol 27(2):132–136
45. Li SH, Zhu HG, Wang J, Jin GM, Gu YF, Liu DY (2009) Effect of environmental estrogen boron on microstructure of thymus in rats. Journal of Anhui Science & Technology University (6):1–5
46. Henderson K, Stella SL, Kobylewski S, Eckhert CD (2009) Receptor activated Ca(2+) release is inhibited by boric acid in prostate cancer cells. PLoS One 4(6):e6009
47. Huang HB, Xiao K, Lu S, Yang KL, Ansari AR, Haseeb K, Song H, Zhong JM, Liu HZ, Peng KM (2015) Increased thymic cell turnover under boron stress may bypass TLR3/4 pathway in African ostrich. PLoS One 10(6):e0129596
48. Lee MD, Bingham KN, Mitchell TY, Meredith JL, Rawlings JS (2015) Calcium mobilization is both required and sufficient for initiating chromatin decondensation during activation of peripheral T-cells. Mol Immunol 63(2):540–549
49. Li S (2005) Effect of boron on the growth, hematology and development of immune organ in Gushi Chickens (in chinese). Journal of Northwest A&F University 37(2):52–58
50. Goihl J (2002) More research needed on boron supplementation of swine diets. Feedstuffs 74:10–27
51. Macian F (2005) NFAT proteins: key regulators of T-cell development and function. Nat Rev Immunol 5(6):472–484
52. Mcneil LK, Starr TK, Hogquist KA (2005) A requirement for sustained ERK signaling during thymocyte positive selection in vivo. P Natl Acad Sci USA 102(38):13574–13579
53. Khiem D, Cyster JG, Schwarz JJ, Black BL (2008) A p38 MAPK-MEF2C pathway regulates β-cell proliferation. P Natl Acad Sci USA 105(44):17067–17072
54. Barranco WT, Kim DH, Jr SS, Eckhert CD (2009) Boric acid inhibits stored Ca^{2+} release in DU-145 prostate cancer cells. Cell Biol Toxicol 25(4):309–320